Russian Journal of Earth Sciences Online ISSN: 1681-1208

On a Possible Mechanism Forming the Nighttime Maximum of Urban Heat Island Intensity

D. Yu. Demezhko[1], A. A. Gornostaeva[1,*], B. D. Khatskevich[1], and N. R. Fakaeva[1]

[1] Institute of Geophysics, the Urals Branch of Russian Academy of Sciences, Yekaterinburg, Russian Federation
* **Correspondence to:** Anastasiya Gornostaeva, free_ride_@mail.ru

Abstract: In most cities in the world, the daytime maximum of the urban heat island (UHI) intensity is observed after sunset. It is minimal around noon. We propose a new mechanism for the formation of the UHI intensity's diurnal cycle that considers the phase shift between surface temperature variations in the city and surroundings. This phase shift occurs due to the difference in thermophysical structure of the subsurface in urban and rural areas. In the case of a homogeneous medium, the temperature maximum at the surface is observed $\pi/4$ later than the heat flux maximum at solar noon. With the presence of an upper layer having a low thermal conductivity compared to the underlying layers, the phase shift would be less than $\pi/4$. Such conditions are often observed in rural areas. The delay of the temperature variations in the city relative to those in the countryside leads to an even greater delay in the UHI intensity relative to the heat flux. This is probably the main reason for the UHI intensity's diurnal variations being observed. The proposed mechanism was verified through the data obtained at weather stations in Yekaterinburg and its surroundings.

Keywords: urban heat island intensity, diurnal cycle, ground surface heat flux, ground surface temperature, solar radiation, thermal effusivity, thermal inertia

Citation: Demezhko D. Yu., Gornostaeva A. A., Khatskevich B. D., and Fakaeva N. R. (2026), On a Possible Mechanism Forming the Nighttime Maximum of Urban Heat Island Intensity, *Russian Journal of Earth Sciences*, 26, ES3006, EDN: LNOKIY, https://doi.org/10.2205/2026es001065

1. Introduction

The phenomenon of an urban heat island (UHI) in surface air temperature has been known for two centuries [*Howard*, 1818]. It is manifested by warmer surface air temperatures in cities compared to those in rural surroundings [*Lokoshchenko et al.*, 2016; *McBoyle*, 1968; *Rizwan et al.*, 2008]. In the scope of ongoing global warming and more frequent occurrences of heat waves, understanding the causes and patterns of the UHI effect is vital for developing heat mitigation strategies and improving urban development and management policies [*Ao et al.*, 2019; *Founda and Santamouris*, 2017; *Liu et al.*, 2022; *Tan et al.*, 2009].

T. R. Oke defined a heat island as a "nocturnal phenomenon" [*Oke*, 1982]. The daytime maximal of the UHI intensity occurs after sunset. It is minimal around noon in most cities in the world [*Jongtanom et al.*, 2011; *Kim and Baik*, 2002; *Kłysik and Fortuniak*, 1999; *Lai et al.*, 2018; *Liu et al.*, 2022; *Magee et al.*, 1999; *Mao et al.*, 2023; *Scott et al.*, 2018; *Xue et al.*, 2023]. Following T. R. Oke, most researchers explain this fact by the absorption of part of the outgoing night long-wave radiation by the walls of buildings, while in the countryside, nothing hinders the ground surface from cooling rapidly [*Johnson et al.*, 1991; *Liu et al.*, 2007; *Oke et al.*, 1991; *Sobstyl et al.*, 2018].

S. N. Goward pointed out the differences in the thermal properties of urban and rural surfaces as the main reason for the nighttime maximum [*Goward*, 1981]. The influence of thermal effusivity (thermal inertia, thermal admittance) on the diurnal temperature variation was considered in his simplest model. Thermal effusivity E determines the rate of heat transfer at the interface between two media and is related to thermal conductivity λ, density ρ, and specific heat capacity C by the relation $E = (\lambda \rho C)^{1/2}$. The higher thermal effusivity of urban surfaces (asphalt, concrete) in comparison with natural rural ones ensures

Review

Received: December 27, 2024
Accepted: October 6, 2025
Published: July 29, 2026

slower heating of the urban surfaces but also slower cooling. However, the calculations performed by this model contradicted the experimental data, so the author had to account for the thermal inhomogeneities of the media, though only by calculating the apparent thermal effusivity. He also added latent heat transfer from the surface in rural areas to the model, which made the UHI intensity positive throughout the day. Even that did not resolve all the contradictions but led to the conclusion that the diurnal cycle cannot be explained by differences in thermal properties alone [*Stewart et al.*, 2021].

The fallacy in Goward's approach was that he considered the temperature response to an isolated radiation pulse and not to a periodic signal. As will be shown further, thermal effusivity (as it may be) determines only the amplitude of temperature variations under conditions of a homogeneous medium. Temperatures in the city and in the countryside change in phase with each other and with the UHI intensity. Montávez et al. combined mechanisms of the UHI formation proposed by T. R. Oke and S. N. Goward in their model [*Montávez et al.*, 2007]. They showed that the urban canyon structure and the urban-rural difference in thermal properties are the main factors affecting the UHI intensity. However, the model does not explain the timing of the UHI maximum.

Finally, several researchers associate the nighttime UHI maximum with weather and anthropogenic factors with stable diurnal dynamics. For example, with diurnal fluctuations in urban-rural humidity difference. However, the relationship between humidity and air temperature is ambiguous in different regions. Various mechanisms are put forward to explain the established relationship, depending on its sign. The positive relationship is explained by the fact that water vapor in the atmosphere delays outgoing long-wave radiation from the surface. Urban humid atmosphere increases the sky's long-wave irradiance over the city and additionally heats the ground surface [*Holmer and Eliasson*, 1999; *Kobayashi*, 1982; *Lindgren*, 1997]. Several mechanisms are considered to explain the negative relationship. 1) More intensive evaporation from the rural surface, where soil humidity is higher, leads both to the vapor pressure increase and the temperature decrease [*Kim and Baik*, 2002]. 2) Under the same urban and rural water vapor content, relative humidity is higher in areas with lower temperatures [*Liu et al.*, 2007]. The latter explanation suggests that not humidity differences, as they are, cause the UHI, but just the opposite. Demin et al. associate the nighttime maxima recorded in Moscow during the cold season at weather stations located at high elevations with the descent of cold air from the hills to the lowlands [*Demin et al.*, 2018]. Some researchers explain diurnal variations in the UHI by the cyclical nature of human activity. Jongtanom et al. noted higher nighttime activity in cities compared to rural areas and, hence, higher heat generation at night [*Jongtanom et al.*, 2011]. Aslam et al. and Kulmala et al. associate the daytime relative decrease in urban areas with an increased content of pollutants that prevent the entry of long-wave radiation [*Aslam et al.*, 2017; *Kulmala et al.*, 2023].

There is no doubt that all these factors play a significant role in different climatic conditions. However, the prevalence of the "nocturnal phenomenon" of the UHI in all climatic zones of the world suggests the presence of a more universal mechanism for its formation.

We propose a new possible mechanism forming the UHI diurnal cycle, accounting for the differences in phase shifts of temperature courses in the city and in the countryside relative to astronomical noon. The differences, for their part, are determined not by the thermal properties of the medium where the heat exchange occurs but by their inhomogeneities.

2. The Model

The proposed mechanism for the formation of the diurnal course of the UHI intensity involves two simplifications:

1. The surface air temperature is determined mainly by heat exchange with the ground surface and, consequently, by the ground surface temperature. This dependence can be disturbed by the influence of wind, atmospheric precipitation, and moisture evaporation, but it certainly plays a crucial role on clear windless days [*Yoshino*, 1975].

In temperate climates, the diurnal variations of the surface air temperature and the ground surface temperature show similar patterns in the four seasons, but they are especially close in spring and summer in calm weather [*Wen et al.*, 2023].

2. Changes in the ground surface heat flux occur in phase with variations in solar radiation [*Demezhko et al.*, 2022], and the heat flux amplitude is proportional to the amplitude of solar radiation. The proportionality factor depends on the surface albedo, humidity, and evaporation rate.

Diurnal variations of the UHI intensity are formed by successive transformations (Figure 1).

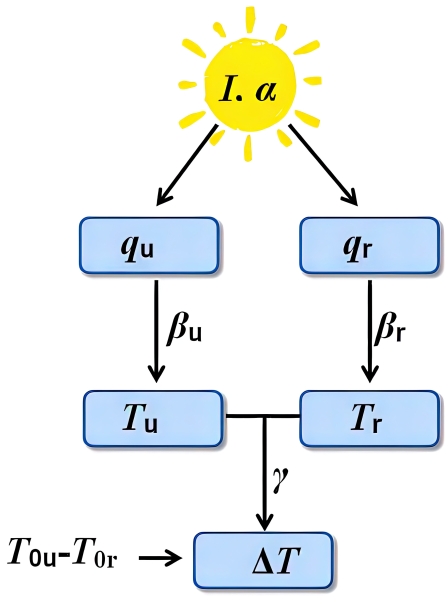

Figure 1. Scheme of the formation of the diurnal cycle of the UHI intensity.

Here I is incoming radiation, q is the ground surface heat flux, T_u and T_r are, respectively, variable components of the ground surface temperature in urban and rural areas, ΔT is a variable component of the UHI intensity, ΔT_0 is a constant component of the UHI intensity equal to the difference in mean daily temperatures $T_{0u} - T_{0r}$, α, β, γ are phase shifts. The ground surface heat flux and solar radiation vary synchronously [*Demezhko et al.*, 2022]. Diurnal variations of incoming radiation I generate the surface heat flux variations q and, in turn, fluctuations in the ground surface temperature. Harmonics of temperature variations lag the corresponding harmonics of surface heat flux variations by the value of β, which depends on the thermal inhomogeneities of the subsurface and frequency. Variations of the UHI intensity are determined by the difference in instantaneous temperatures in the city and rural surroundings ($\Delta T = T_u - T_r$). Therefore, the amplitude and phase of the UHI are accordingly determined by the amplitudes and phase differences of surface temperature variations in urban and rural areas.

3. Lag of Temperature Variations from Surface Heat Flux Variations

For simplicity, let us consider the transformation of the fundamental 24-hour harmonic of the surface heat flux variations, assuming the conclusions obtained are also valid for higher harmonics of radiation origin. The surface heat flux variations are described by the dependence:

$$q(t) = A_q \cos(\omega t - \alpha),$$

where A_q is the amplitude, $\omega = 2\pi/24$ hours^{-1} is the frequency, and α is the initial phase. Since the heat flux reaches its maximum at solar noon, $\alpha = \pi$. The ground surface temperature variations lag the heat flux variations by β:

$$T(t) = T_0 + A_T \cos(\omega t - \alpha - \beta), \tag{1}$$

where T_0 is the mean daily surface temperature. In a homogeneous half-space, $\beta = \pi/4$, i.e., 1/8 of the oscillation period [*Bennet et al.*, 2008; *Carslaw and Jaeger*, 1959]. In absolute terms, this lag depends on the oscillation period. It equals 3 hours for a 24-hour harmonic, 1.5 hours for a 12-hour harmonic and an hour for an 8-hour harmonic. If the total solar radiation maximum and the maximum of the surface heat flux are observed simultaneously at the solar noon, the temperature maximum of the main 24-hour harmonic will be observed 3 hours later. Note that the phase shift value does not depend on the thermal properties in contrast to the amplitude of temperature variations at the surface of a homogeneous half-space:

$$A_T = \frac{A_q}{E\omega^{1/2}}, \tag{2}$$

where E is the thermal effusivity (thermal inertia), $E = (\lambda\rho C)^{1/2} = \lambda/a^{1/2}$, λ is the thermal conductivity, ρ is the density, C is the specific heat capacity, and a is the thermal diffusivity. Thermal effusivity, also known as thermal inertia, thermal admittance or thermal responsivity, is a measure of a material's ability to exchange energy with surroundings. The amplitude of temperature variations is directly proportional to the amplitude of the surface heat flux and inversely proportional to the thermal effusivity of the soil E and the root of the frequency. The latter determines the smaller contribution of the higher harmonics present in the heat flux variations to temperature variations.

The lag of the temperature curve will differ from $\pi/4$ in the case of vertical heterogeneity, for example, a horizontally layered medium. The amplitude under these conditions can no longer be determined in terms of a single thermal parameter, for example, thermal effusivity. The solution to this problem for a layered inhomogeneous medium was obtained in [*Byrne and Davis*, 1980] within the concept of "complex thermal admittance". The monograph [*Demezhko*, 2001] presents a solution to the problem of propagation of harmonic temperature oscillations from the surface to the depth if the upper contrasting layer of thickness h lies on a layer of infinite thickness. Temperature variations in the upper layer at a depth of z will also be described by the harmonic law:

$$T(z,t) = T_0 + A_T(z)\cos(\omega t - \psi(z)). \tag{3}$$

The amplitude $A_T(z)$ and the phase shift $\psi(z)$ of temperature variations in the upper layer at a depth z are described by relations:

$$A_T(z) = A_T(0)\exp(-kz)\left[\frac{1 - 2p_z\cos u_z + p_z^2}{1 - 2p_0\cos u_0 + p_0^2}\right]^{1/2},$$

$$\psi(z) = kz - \arctan\left[\frac{p_z \sin u_z}{1 - 2p_z\cos u_z}\right] + \arctan\left[\frac{p_0 \sin u_0}{1 - 2p_0\cos u_0}\right],$$

where $p_z = \varepsilon\exp(-u_z)$, $u_z = 2k(h - z)$, $p_0 = \varepsilon\exp(-u_0)$, $u_0 = 2kh$, $k = (\omega/2a)^{1/2}$, ε is the thermal contrast parameter:

$$\varepsilon = \frac{E_2 - E_1}{E_2 + E_1}. \tag{4}$$

Thermal effusivity E_1 refers to the upper layer, while E_2 refers to the lower one. Having numerically differentiated (3) with respect to depth, we find the variations of the surface heat flux:

$$q(0,t) = -\lambda\frac{\mathrm{d}T(z,t)}{\mathrm{d}z}. \tag{5}$$

Comparing variations of temperature and heat flux at the surface, let us estimate the ratio of their amplitudes A_T/A_q and the phase shift β in relation (1). They depend on the thermal diffusivity of the upper layer and the thermal contrast ε expressed in terms of the thermal effusivities of the two media. Thermal conductivity in (5) can also be expressed in terms of these parameters: $\lambda = E_1 a^{1/2}$. Since the thermal conductivity, density, and specific heat capacity of unlithified soils increase as humidity rises, the thermal diffusivity $a = \lambda/\rho C$ changes insignificantly. With that in mind, we can express the dependencies of the phase shift β and the amplitude of temperature variations A_T on the thickness of the upper layer h and thermal contrast ε (Figure 2).

The lag of the temperature curve from the heat flux change curve will differ from $\pi/4$. $\beta < \pi/4$ if the upper layer has a lower thermal effusivity compared to the lower one, and $\beta > \pi/4$ if the thermal effusivity of the upper layer is higher (Figure 2a). Curves $\beta(h)$ have extrema. The maximal effect is observed at the thickness of the upper layer $h_{\text{eff}} \approx 0.06L$, where $L = 2\pi(2a/\omega)^{1/2}$ is the wavelength. Indeed, for a diurnal wave $L = 1$ m (at $a = 1\times10^{-6}$ m^2/s), the maximal deviation from $\pi/4$ in phase shift will be observed under $h_{\text{eff}} \approx 6$ cm. The effective thickness will be smaller for higher harmonics, i.e., $h_{\text{eff}} = 4.2$ cm for a semi-diurnal harmonic, and $h_{\text{eff}} = 3.5$ cm for an 8-hour harmonic. An overly thin ($h < 0.5\times10^{-3}L$) or, on the contrary, an overly thick ($h > 0.5L$) layer does not affect the phase shift; like in the simplest model, it remains equal to $\pi/4$. The higher the deviation of the phase shift from $\pi/4$, the greater the thermal contrast of the layers.

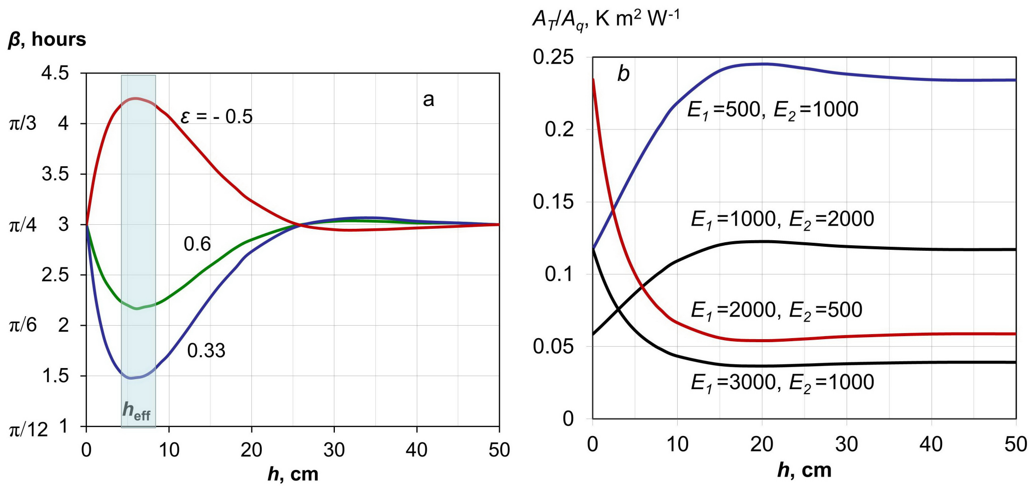

(a) (b)

Figure 2. Dependence of the phase shift between variations of the surface heat flux and the surface temperature (a) and the ratio of the amplitude of temperature variations to that of heat flux variations on the thickness of an upper layer h that is anomalous in terms of thermal properties. Codes of curves: (a) – the thermal contrast of two media, (b) – the thermal effusivity, J/(m^2 K s$^{1/2}$).

The amplitude of temperature fluctuations depending on the thickness h predictably varies between the values determined by formula (2) for the thermal effusivities of the upper and lower layers (Figure 2b). For a diurnal wave under a thickness of the upper layer $h > 15$ cm, the amplitude at the surface is almost completely determined by the thermal effusivity E_1.

Assemblages of curves in Figure 2 can be reduced to one or two curves by introducing dimensionless phase $f_\beta(h)$ and amplitude $f_A(h)$ functions (Figure 3). Then the real phase and amplitude can be calculated as

$$\beta = \frac{\pi}{4}(1 - \varepsilon f_\beta), \tag{6}$$

$$A_T(E_1, E_2) = A_T(E_2) + f_A[A_T(E_1) - A_T(E_2)], \tag{7}$$

where $A_T(E_1)$ and $A_T(E_2)$ are amplitudes of temperature variations at the surface of a homogeneous half-space with thermal effusivities E_1, E_2.

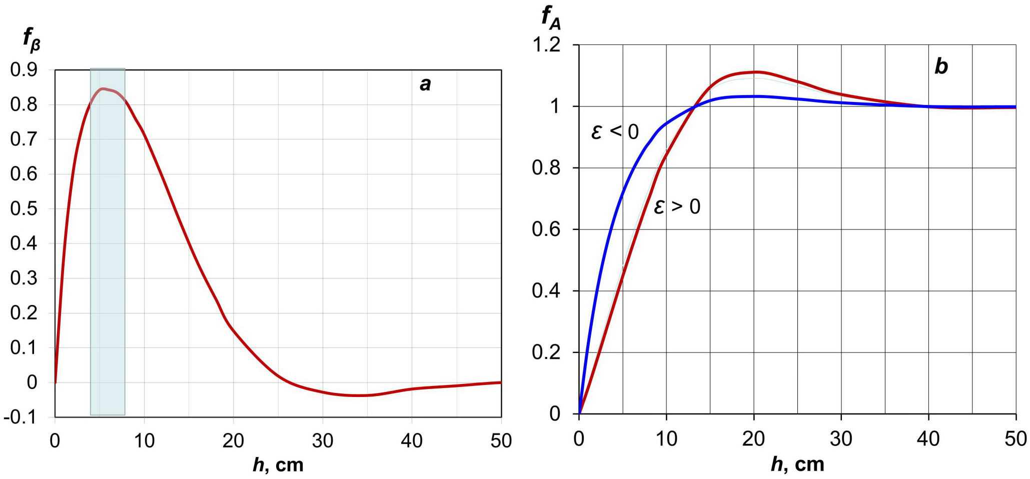

(a) (b)

Figure 3. The dependences of the (a) phase and (b) amplitude functions on the thickness of the upper anomalous layer.

4. Phase Shift Between Temperature and UHI Intensity Variations

If urban and rural soils were homogeneous (even with different values of thermal properties in urban and rural areas) or equally heterogeneous, then surface temperatures would vary synchronously in the city and surroundings, and the maximal UHI intensity would be observed simultaneously with the temperature maximum. However, differences in surface thermal inhomogeneities in urban and rural areas lead to differences in phase shifts of temperature variations ($\beta_u \neq \beta_r$). The phase γ of diurnal variations of the UHI intensity ΔT will naturally differ from phases of urban and rural temperature curves:

$$\begin{gathered}\Delta T(t) = T_u - T_r = \\ T_{0u} - T_{0r} + A_{Tu}\cos(\omega t - \alpha - \beta_u) - A_{Tr}\cos(\omega t - \alpha - \beta_r) = \\ T_{0u} - T_{0r} + A_\Delta \cos(\omega t - \alpha - \beta_u - \gamma),\end{gathered} \tag{8}$$

where T_{0u} and T_{0r} are the mean daily temperatures in urban and rural areas, respectively. The phase γ counted from the urban temperature curve and the amplitude A_Δ are determined by relations:

$$\tan(\gamma) = \frac{\sin(\beta_u - \beta_r + \pi)}{\frac{A_u}{A_r} + \cos(\beta_u - \beta_r + \pi)}, \tag{9}$$

$$A_\Delta = A_u\left[1 + \left(\frac{A_u}{A_r}\right)^2 + 2\frac{A_u}{A_r}\cos(|\beta_u - \beta_r| + \pi)\right]^{1/2}. \tag{10}$$

The amplitude of the UHI intensity A_Δ does not depend on the sign of the phase difference of the temperature curves but depends on the ratio of their A_u/A_r amplitudes. The phase of the ΔT curve is positive ($\gamma > 0$, i.e., ΔT lags temperature curves) if the rural curve is ahead of the urban one ($\beta_u - \beta_r > 0$) and vice versa (Figure 4a). The amplitude of the UHI intensity A_Δ grows linearly with an increase in $|\beta_u - \beta_r|$ in the case of equal amplitudes of the initial curves ($A_u/A_r = 1$) (Figure 4b).

5. Synthetic Example

In rural landscapes, the upper layer enriched with organic matter (sod, needles, leaves, arable land) lies on loams and sandy loams, whose thermal conductivity is about twice as high. Thermal effusivities relate to each other in approximately the same ratio.

Urban areas are laterally less homogeneous. There are asphalt roads here containing layers of asphalt-concrete 8–15 cm thick (λ = 1.4–1.8 W m^{-1} K^{-1}, see, e.g., [*Stempihar et al.*,

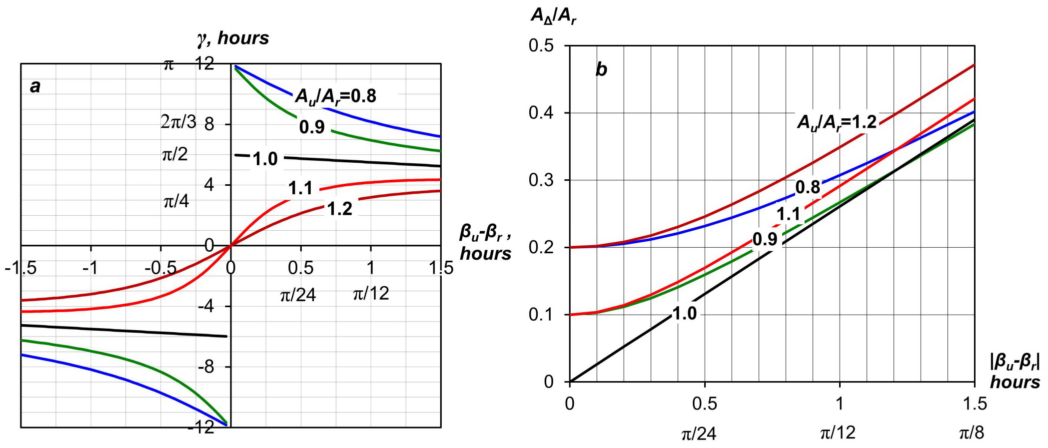

(a) (b)

Figure 4. The phase shift γ of the UHI intensity relative to urban temperature variations (a) and the relative amplitude A_Δ/A_r of the UHI intensity (b) depending on the phase difference $\beta_u - \beta_r$ and the ratio of the A_u/A_r amplitudes of temperature variations in urban and rural areas.

2012]) lying on a crushed stone-sand base up to 1 m thick. In natural water saturation, the thermal conductivity of this layer fluctuates within approximately the same limits as that of the asphalt surface. If the asphalt layer lies on a dry base with low thermal conductivity, then the phase shift of the diurnal variation of the surface temperature will be opposite to the rural situation, i.e., $\beta_u > \pi/4$ (> 3 hours for a 24-hour harmonic). The same can be said about concrete roof slabs, under which there is a layer of thermal insulation. However, there are also parks and lawns in the city where the ratio of thermal properties is the same as in the countryside.

Air temperature recorded at meteorological stations at a height of 2 m is formed by the heat exchange over an area that is much larger than the size of the meteorological site. This area may include territories with different thermal properties and different types of vertical heterogeneity. That means that one can talk about thermal differences between urban and rural areas only "on average". It is practically impossible to compile a statistically weighted "thermophysical portrait" of the city under these conditions. Therefore, in this section we will illustrate the model for the case where the urban environment is usually more homogeneous than the rural one, and surface temperature variations in the city will lag those in the countryside ($\beta_u > \beta_r$). The model verification using meteorological data will be carried out below in the Section "The Model Validation and Discussion". If the observed phase shift of a 24-hour harmonic of the surface air temperature variations will occur close to 3 hours, then the diurnal temperature cycle was formed under conditions of a homogeneous (on average) vertical thermophysical section.

Let us estimate the diurnal variation of the 24-hour harmonic of the UHI intensity under conditions close to real ones (Table 1). For simplicity, we assume the amplitude of the diurnal wave of surface heat flux A_q to be the same in urban and rural areas.

Figure 5 shows the calculation results. The surface heat flux reaches its maximum at solar noon, simultaneously with the maximum of incoming solar radiation. With the presence of an upper layer with low thermal effusivity, the surface temperature maximum in the countryside lags the heat flux maximum by 2.2 hours. The surface temperature maximum in the city lags the heat flux maximum by 3 hours, as in a homogeneous medium.

Note that the amplitude of temperature variations in the city is lower than in the countryside due to the higher thermal effusivity of urban surfaces. The phase difference $\beta_u - \beta_r = 0.8$ hours and the amplitude ratio $A_{Tu}/A_{Tr} = 0.75$ ensure the diurnal variation of the UHI intensity with a nighttime maximum at $\alpha + \beta_r + \gamma = 12 + 3 + 8.7 = 23.7$ hours and the amplitude equal to $A_\Delta = 4.3$ K.

Table 1. The diurnal variation of the 24-hour harmonic of the UHI intensity under conditions close to real ones. Input parameters are colored green

Surface heat flux variation					
Urban			Rural		
Parameter	Value		Parameter	Value	
A_q, W/m^2	150		A_q, W/m^2	150	
α, hours	12.0		α, hours	12.0	
Surface temperature variation					
Parameter	Value	Equation	Parameter	Value	Equation
E, J/(m^2 K s$^{1/2}$)	1600		E_1, J/(m^2 K s$^{1/2}$)	1000	
ΔT_u, K	11.0	(2)	E_1, J/(m^2 K s$^{1/2}$)	2000	
a, m^2/s	$1 \cdot 10^{-6}$		$a_1 = a_2$, m^2/s	$1 \cdot 10^{-6}$	
β_u, hours	3.00	(1)	ε	0.33	(4)
			h, m	0.08	
			f_β	0.80	Figure 3a
			β_r, hours	2.20	(6)
			f_A	0.75	Figure 3b
			ΔT_r, K	14.4	(7)
UHI intensity variation					
Parameter	Value	Equation			
$\beta_u - \beta_r$, hours	0.80				
$\Delta T_u / \Delta T_r$, K	0.77				
γ, hours	8.71	(9)			
A_Δ, K	4.3	(10)			

6. The Model Validation and Discussion

The presented model describes the UHI forming in a diurnal cycle in terms of ground (pavement) surface temperatures. Is this model suitable for describing the UHI in terms of surface air temperatures? To answer this question, we used minute-resolution surface air temperature data recorded in August 2022 at weather stations in the center of Yekaterinburg (56.83°N, 60.63°E) and in Verkhnee Dubrovo village located 28 km southeast (56.73°N, 61.07°E). The Yekaterinburg weather station is located in the central part of the city on a hilltop surrounded by a park (Figure 6). According to the concept of Local Climatic Zones (LCZ) [*Stewart and Oke*, 2012], this place can be classified as LCZ-4 (open arrangement of tall buildings to tens of stories, abundance of pervious land cover – low plants, scattered trees). However, recent studies conducted in Moscow [*Varentsov et al.*, 2021] have shown that the spatial heterogeneity of the UHI intensity is not so much determined by local factors described within the LCZ classification as by mesoscale drivers operating within a radius of 2–20 km. Thus, it can be assumed that the data on surface air temperature recorded at the Yekaterinburg weather station on a small hill characterizes the entire central part of the city.

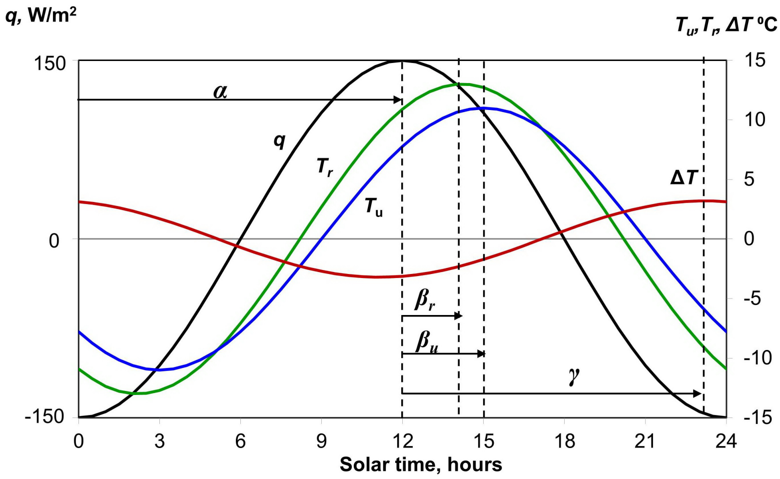

Figure 5. The diurnal variation of the 24-hour harmonics of the surface heat flux (black curve), the ground surface temperature in urban (blue curve) and rural (green curve) areas, and the UHI intensity (red curve) under conditions close to real ones.

(a) (b)

Figure 6. Location of weather station sites in Yekaterinburg (a) and Verkhnee Dubrovo (b) (photo by Dmitry Demezhko and Vyacheslav Bukharov).

The weather station in Verkhnee Dubrovo is classified as LCZ-D (featureless landscape of grass or herbaceous plants; few or no trees; zone function is natural grassland, agriculture, or urban park), partly as LCZ-A (heavily wooded landscape of deciduous trees; land cover, mostly pervious).

Figure 7 shows diurnal surface air temperature changes averaged over the first two decades of August 2022, the driest period of that summer (6 mm of precipitation in Yekaterinburg, 0.6 mm in Verkhnee Dubrovo). The UHI intensity demonstrates a classical form of variation with a nighttime maximum of 3 K and a daytime minimum of 0.5 K at a mean daily value of $\Delta T_0 = 1.6$ K.

The 24-hour harmonic (Table 2) is responsible for most of the diurnal variability of air temperatures and UHI intensity. The temperature maximum at the first harmonic is observed at 4:01 p.m. local time in Yekaterinburg and at 3:28 p.m. in Verkhnee Dubrovo. The lag of maxima from the solar noon (1:04 p.m.) amounts to 2 hours 57 minutes and 2 hours 24 minutes, respectively. A nearly three-hour lag of temperature variations in Yekaterinburg ($\pi/4$) indicates that the heat transfer here occurs at the surface of a homogeneous medium. Less lag (by 33 minutes) and a higher amplitude of temperature fluctuations in Verkhnee Dubrovo indicate the presence of an upper layer with reduced thermal properties. It was confirmed by the thermal conductivity measurements carried out in July–August 2020 [*Demezhko et al.*, 2022]. An approximately 10-cm-thick upper

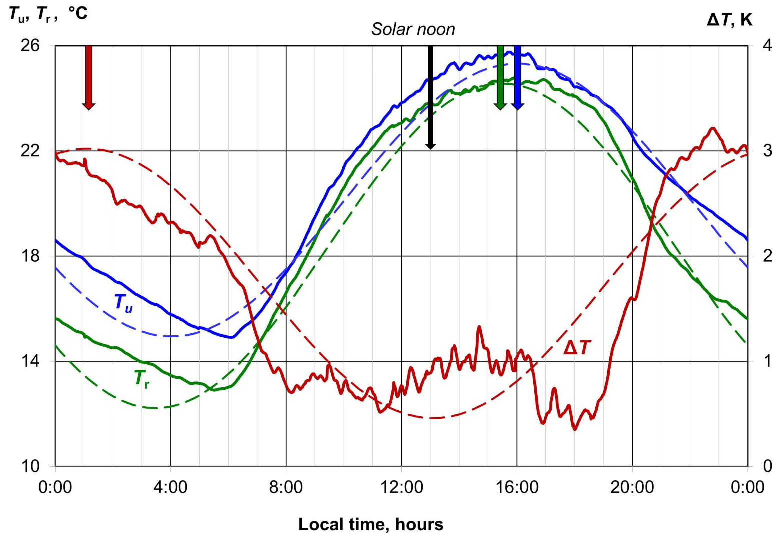

Figure 7. Surface air temperature changes in a diurnal cycle in Yekaterinburg (T_u) and Verkhnee Dubrovo (T_r) averaged over the first two decades of August 2022 (solid lines) and UHI intensity (ΔT). Dotted lines show 24-hour harmonics. The colored arrows mark the maxima of the corresponding harmonics; the black one marks the solar noon.

turf layer with a thermal conductivity of 0.8 W m^{-1} K^{-1} in dry July and 1.1 W m^{-1} K^{-1} in wetter August 2020 lies on loams with a thermal conductivity of 1.5–2.3 W m^{-1} K^{-1}.

The phase differences between the urban and rural 24-hour temperature harmonics lead to the fact that the UHI intensity maximum of the 24-hour harmonic occurs at 1:06 a.m. of the next day, or 9 hours and 1 minute later than the urban temperature maximum.

Thus, the described model explains the 24-hour component of diurnal variations in the UHI intensity in Yekaterinburg in terms of surface air temperature quite well. Since impenetrable urban pavements are typical for most cities in the world, just as upper soil layers with reduced thermal properties are a feature of suburban areas, the described model seems to be quite universal.

In addition to the 24-hour harmonic, the UHI intensity diurnal variations contain a local afternoon maximum and local morning and evening minima (Figure 7). The morning minimum, when ΔT sometimes reaches negative values (the so-called urban cool island, or UCI), is observed in some cities. It is explained by the influence of the geometry of cities (the canyon effect) that hinders direct morning insolation of the surface [*Earl et al.*, 2016; *Oke*, 1982]. It is possible that the canyon effect is also responsible for the evening minimum. The local afternoon maximum is not a unique phenomenon either. A similar maximum was observed, for example, in Delhi [*Aslam et al.*, 2017], Athens [*Founda and Santamouris*, 2017], and Shanghai [*Ao et al.*, 2019], but no convincing explanation was provided.

Spectral decomposition of temperature data revealed 12-hour and 8-hour harmonics both in Yekaterinburg and Verkhnee Dubrovo (Table 2). For an 8-hour harmonic, the phase difference between temperature variations in the city and in the countryside in radian terms is approximately the same as for 24-hour harmonics. The 8-hour harmonic amplitude in Yekaterinburg is lower than in Verkhnee Dubrovo. It suggests that the 8-hour harmonic is of radiative origin, and its transformation happens due to the same mechanism as the transformation of the 24-hour harmonic. The phase shift between the city and the countryside for the 12-hour harmonic is excessively large, while the amplitude ratio $A_{T\mathrm{u}}/A_{T\mathrm{r}} > 1$, which indicates a different mechanism of its formation, for example, through evapotranspiration or the canyon effect. At the same time, both the 8-hour and 12-hour harmonics of ΔT form the daytime local maximum, and the 8-hour harmonic forms the local morning and evening minima as well (Figure 8).

The UHI intensity in the diurnal cycle is everywhere positive. It is due to differences in mean daily temperatures: 20.1°C in Yekaterinburg and 18.4°C in Verkhnee Dubrovo. A higher mean daily temperature in the city is obviously associated with factors that

Table 2. Summary of spectral analysis of surface air temperatures in Yekaterinburg (T_u) and Verkhneye Dubrovo (T_r) in August 2022

Harmonic, hours	Location	Amplitude, K	Local time of maximum	Phase diff. $\beta u - \beta r$		ΔT phase shift $\gamma u - \gamma r$	
				rad.	min.	rad.	hours
24	Yekaterinburg	5.18	4:01 p.m.	0.144	33	2.38	9.09
	V. Dubrovo	6.17	3:28 p.m.				
12	Yekaterinburg	0.63		0.661	76		
	V. Dubrovo	0.36					
8	Yekaterinburg	0.56		0.157	12		
	V. Dubrovo	0.82					

constantly operate during the day, for example, the obstruction of the outgoing long-wave radiation in the city. Although the traditional explanation of the variable component with a nighttime UHI maximum suggests the nighttime obstruction of the outgoing radiation in the city, it is easy to make sure that this is not the case. It suffices to consider the diurnal behavior of the outgoing radiation recorded by actinometric stations. For example, in Verkhnee Dubrovo in July 2020, the diurnal intensity of outgoing long-wave radiation varied from 400 W/m^2 at night to 500 W/m^2 during the day [*Demezhko et al.*, 2022]. The temperature effect in the city caused by this factor will be proportional to the intensity of the outgoing radiation, i.e., a little higher during the day. Other factors leading to an increase in the long-term surface temperature in the city are permanent heat sources, reduced evapotranspiration, and albedo.

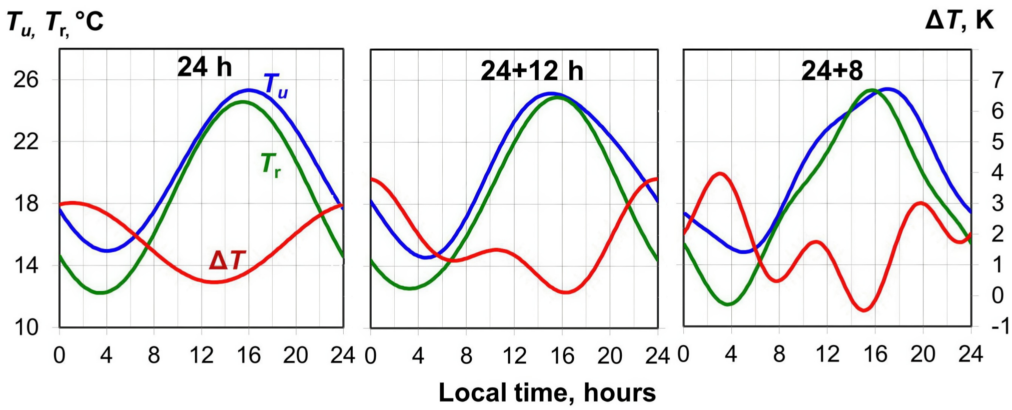

Figure 8. The diurnal cycle of temperatures in Yekaterinburg (T_u) and Verkhneye Dubrovo (T_r) synthesized from the first three harmonics and the UHI changes (ΔT).

The given example for August 2022, when the a priori simplifications adopted in the model (see section "The Model") were observed almost perfectly, showed that in such conditions the model explains the diurnal variation of the UHI well. Let's consider the model's validity in other seasons. Table 3 shows the characteristics of 24-hour harmonics of diurnal air temperature variations in Yekaterinburg and V. Dubrovo, averaged over the months of 2023. The characteristics were calculated using spectral analysis of temperature data from a 3-hour sampling (https://rp5.ru/).

The temperature maximum of the 24-hour harmonic in Yekaterinburg is observed at 3:54–5:48 p.m. and in V. Dubrovo at 3:24–5:27 p.m. Moreover, in all months, the temperature maximum in Yekaterinburg is observed 5–80 minutes later than the temperature maximum in V. Dubrovo. A lag close to 30 minutes, as in the "ideal" example discussed above, is typical for the warm half of the year (April–October). The large spread of $\beta_u - \beta_r$ estimates and the low amplitude of temperature variations in November–March indicates

Table 3. Characteristics of the 24-hour harmonic of the diurnal variation of air temperatures in Yekaterinburg and V. Dubrovo and the 24-hour harmonic of UHI intensity in 2023

Months	Temperature variation				Phase diff. $\beta_u - \beta_r$, min	UHI intensity		
	Yekaterinburg		V. Dubrovo					
	Loc. time of maximum	Amplitude, K	Loc. time of maximum	Amplitude, K		Loc. time of maximum	Amplitude, K	R^2
Jan	05:48 p.m.	0.87	04:28 p.m.	0.94	80	11:58 p.m.	0.32	0.54
Feb	04:38 p.m.	2.53	04:17 p.m.	2.67	21	00:35 a.m.	0.27	0.38
Mar	04:15 p.m.	2.49	03:56 p.m.	2.72	19	01:16 a.m.	0.31	0.75
Apr	04:28 p.m.	4.58	03:53 p.m.	4.85	35	11:32 p.m.	0.77	0.79
May	04:03 p.m.	5.64	03:30 p.m.	6.10	33	11:41 p.m.	0.97	0.82
Jun	03:56 p.m.	4.04	03:24 p.m.	4.49	32	00:09 a.m.	0.74	0.66
Jul	03:54 p.m.	4.30	03:31 p.m.	4.44	23	10:53 p.m.	0.46	0.58
Aug	04:16 p.m.	3.76	03:40 p.m.	4.19	36	00:14 a.m.	0.76	0.98
Sep	04:09 p.m.	3.80	03:25 p.m.	3.63	44	08:52 p.m.	0.73	0.79
Oct	04:13 p.m.	1.64	03:43 p.m.	1.67	30	10:32 p.m.	0.21	0.78
Nov	04:35 p.m.	0.62	04:18 p.m.	0.85	17	07:16 p.m.	0.10	0.22
Dec	05:32 p.m.	0.58	05:27 p.m.	0.40	5	05:41 p.m.	0.18	0.33

an insignificant influence of solar radiation on the surface air temperature. The maximum of the UHI (ΔT) is observed at 17:41 p.m.–01:16 a.m. of the next day. The maximal amplitude of the daytime UHI intensity is observed in April–September. The coefficient of determination (R^2) presented in the last column of Table 3 measures which part of the observed dispersion of the diurnal variations of ΔT is determined by the 24-hour harmonic. The coefficient of determination consistently exceeds 0.5 in the warm half of the year, and it is minimal in the winter months. During this period, there are a minimum number of clear days in the Urals. Snow cover also prevents radiation heat transfer. Thus, as it has been expected, the described model explains well the nighttime maximum of the diurnal UHI variations in the warm half of the year with the maximum number of clear days.

7. Conclusions

A new possible mechanism that explains the typical pattern of the diurnal UHI intensity cycle with a nighttime maximum and a daytime minimum considers the phase shift between the temperature variations in urban and rural areas. This phase shift occurs due to the difference in thermal structure of the subsurface in the city and countryside. The insolation maximum and the maximum of the ground (pavement) surface heat flux are simultaneously observed at solar noon. In the case of a homogeneous medium, the maximal temperature at the surface is observed $\pi/4$ later than the heat flux maximum (i.e., 3 hours later for the main 24-hour harmonic). With the presence of an upper layer having low thermal properties compared to the underlying layers (for example, turf lying on loam), the phase shift between the heat flux and temperature variations would be less than $\pi/4$. Such conditions are often observed in rural areas, leading to a decrease in the phase shift between the heat flux and temperature in the countryside compared to the values in the city. The delay of temperature variations in the city relative to those in the countryside leads to an even greater delay in their difference (the UHI intensity) relative to the heat flux. For the 24-hour harmonic, this additional delay will be approximately 6 hours, or 9 hours from the solar noon under equal rural and urban amplitudes of diurnal temperature variations. The proposed mechanism is most efficient in calm weather with its clear skies and low wind speed when the net radiation plays the main role.

The model's validity was proven by a single example, that of Yekaterinburg. In addition to the described mechanism, meteorological factors that have stable diurnal dynamics in certain seasons, such as wind, precipitation, and processes occurring in the boundary layer, can contribute to the formation of the diurnal cycle of the UHI. The height of the convective boundary layer that is usually less at night determines the relation between the air surface and the ground surface temperatures and may introduces natural distortions into the described mechanism.

Because a nocturnal UHI maximum is a common phenomenon, further testing of the model should be carried out using high-resolution meteorological data from other cities of various sizes, located in different geographical situations. That is the subject of future research.

The described mechanism determines the variable part of the diurnal UHI intensity. The permanent part is formed by the higher mean daily temperatures in the city. They can be associated with excessive heat accumulation in the underground environment due to permanent urban heat sources, reduced evaporation, and the low albedo of the urban surface.

Because the UHI factor contributes crucially to global warming, heat related mortalities, and unpredictable climatic changes, it is very important to identify the main causes of the UHI. We hope that the model we have developed will contribute to a better understanding of the mechanisms of the urban heat island formation.

Acknowledgments. This work was funded by the Russian Science Foundation (project No. 22-77-10018, https://rscf.ru/project/22-77-10018/).

References

Ao X., Wang L., Zhi X., et al. Observed synergies between urban heat islands and heat waves and their controlling factors in Shanghai, China // Journal of Applied Meteorology and Climatology. — 2019. — Vol. 58, no. 9. — P. 1955–1972. — https://doi.org/10.1175/jamc-d-19-0073.1

Aslam M. Y., Krishna K. R., Beig G., et al. Seasonal Variation of Urban Heat Island and Its Impact on Air-Quality Using SAFAR Observations at Delhi, India // American Journal of Climate Change. — 2017. — Vol. 06, no. 02. — P. 294–305. — https://doi.org/10.4236/ajcc.2017.62015

Bennet W. B., Wang J. and Bras R. L. Estimation of global ground heat flux // Journal of Hydrometeorology. — 2008. — Vol. 9, no. 4. — P. 744–759. — https://doi.org/10.1175/2008jhm940.1

Byrne G. F. and Davis J. R. Thermal inertia, thermal admittance, and the effect of layers // Remote Sensing of Environment. — 1980. — Vol. 9, no. 4. — P. 295–300. — https://doi.org/10.1016/0034-4257(80)90035-8

Carslaw H. S. and Jaeger J. C. Conduction of Heat in Solids. — 2nd. — Clarendon Press, 1959. — P. 510.

Demezhko D. Y. Geothermal Method for Paleoclimate Reconstruction (Examples From the Urals, Russia). — Ekaterinburg, Russia : Russian Academy of Sciences, Urals Branch, 2001. — 143 p. — (In Russian).

Demezhko D. Y., Gornostaeva A. A. and Antipin A. N. An assessment of phase relationships between heat fluxes and ground surface temperatures in a diurnal cycle based on monitoring studies at the Verkhnee Dubrovo meteorological station // Lithosphere (Russia). — 2022. — Vol. 22, no. 2. — P. 239–250. — https://doi.org/10.24930/1681-9004-2022-22-2-239-250 — (In Russian).

Demin V. I., Kuznetsova I. N., Brusova N. E., et al. Orographic effects on calculation of the urban heat island intensity // Optika atmosfery i okeana. — 2018. — Vol. 31, no. 2. — P. 128–135. — https://doi.org/10.15372/AOO20180208 — (In Russian).

Earl N., Simmonds I. and Tapper N. Weekly cycles in peak time temperatures and urban heat island intensity // Environmental Research Letters. — 2016. — Vol. 11, no. 7. — P. 074003. — https://doi.org/10.1088/1748-9326/11/7/074003

Founda D. and Santamouris M. Synergies between Urban Heat Island and Heat Waves in Athens (Greece), during an extremely hot summer (2012) // Scientific Reports. — 2017. — Vol. 7, no. 1. — https://doi.org/10.1038/s41598-017-11407-6

Goward S. N. Thermal behavior of urban landscapes and the urban heat island // Physical Geography. — 1981. — Vol. 2, no. 1. — P. 19–33. — https://doi.org/10.1080/02723646.1981.10642202

Holmer B. and Eliasson I. Urban-rural vapour pressure differences and their role in the development of urban heat islands // International Journal of Climatology. — 1999. — Vol. 19, no. 9. — P. 989–1009. — https://doi.org/10.1002/(sici)1097-0088(199907)19:9<989::aid-joc410>3.0.co;2-1

Howard L. The climate of London. Vol. 1. — W. Phillips, 1818. — 221 p.

Johnson G. T., Oke T. R., Lyons T. J., et al. Simulation of surface urban heat islands under 'IDEAL' conditions at night part 1: Theory and tests against field data // Boundary-Layer Meteorology. — 1991. — Vol. 56, no. 3. — P. 275–294. — https://doi.org/10.1007/bf00120424

Jongtanom Y., Kositanont C. and Baulert S. Temporal variations of urban heat island intensity in three major cities, Thailand // Modern Applied Science. — 2011. — Vol. 5, no. 5. — P. 105–110. — https://doi.org/10.5539/mas.v5n5p105

Kim Y.-H. and Baik J.-J. Maximum Urban Heat Island Intensity in Seoul // Journal of Applied Meteorology. — 2002. — Vol. 41, no. 6. — P. 651–659. — https://doi.org/10.1175/1520-0450(2002)041<0651:muhiii>2.0.co;2

Kłysik K. and Fortuniak K. Temporal and spatial characteristics of the urban heat island of Łódź, Poland // Atmospheric Environment. — 1999. — Vol. 33, no. 24/25. — P. 3885–3895. — https://doi.org/10.1016/s1352-2310(99)00131-4

Kobayashi M. Influence of urbanized atmosphere on longwave radiation field at night // Geographical Review of Japan. — 1982. — Vol. 55, no. 6. — P. 421–444.

Kulmala M., Kokkonen T., Ezhova E., et al. Aerosols, clusters, greenhouse gases, trace gases and boundary-layer dynamics: on feedbacks and interactions // Boundary-Layer Meteorology. — 2023. — Vol. 186, no. 3. — P. 475–503. — https://doi.org/10.1007/s10546-022-00769-8

Lai J., Zhan W., Huang F., et al. Identification of typical diurnal patterns for clear-sky climatology of surface urban heat islands // Remote Sensing of Environment. — 2018. — Vol. 217. — P. 203–220. — https://doi.org/10.1016/j.rse.2018.08.021

Lindgren J. Nocturnal Incoming Radiation in and Around Göteborg, Sweden : PhD thesis : B93 / Lindgren J. — 1997. — P. 47.

Liu W., Ji C., Zhong J., et al. Temporal characteristics of the Beijing urban heat island // Theoretical and Applied Climatology. — 2007. — Vol. 87, no. 1–4. — P. 213–221. — https://doi.org/10.1007/s00704-005-0192-6

Liu Z., Zhan W., Lai J., et al. Taxonomy of seasonal and diurnal clear-sky climatology of surface urban heat island dynamics across global cities // ISPRS Journal of Photogrammetry and Remote Sensing. — 2022. — Vol. 187. — P. 14–33. — https://doi.org/10.1016/j.isprsjprs.2022.02.019

Lokoshchenko M. A., Korneva I. A., Kochin A. V., et al. Vertical extension of the urban heat island above Moscow // Doklady Earth Sciences. — 2016. — Vol. 466, no. 1. — P. 70–74. — https://doi.org/10.1134/s1028334x16010128

Magee N., Curtis J. and Wendler G. The Urban Heat Island Effect at Fairbanks, Alaska // Theoretical and Applied Climatology. — 1999. — Vol. 64, no. 1/2. — P. 39–47. — https://doi.org/10.1007/s007040050109

Mao Y., Ren G. and Tysa S. K. Urbanization-Induced Diurnal Variation in Short-Duration Rainfall Events in Wuhan, China // Land. — 2023. — Vol. 12, no. 7. — P. 1343. — https://doi.org/10.3390/land12071343

McBoyle G. B. A review of urban climatology // Earth Science Journal. — 1968. — Vol. 2, no. 1. — P. 88–94.

Montávez J. P., González-Rouco J. F. and Valero F. A simple model for estimating the maximum intensity of nocturnal urban heat island // International Journal of Climatology. — 2007. — Vol. 28, no. 2. — P. 235–242. — https://doi.org/10.1002/joc.1526

Oke T., Johnson G., Steyn D., et al. Simulation of surface urban heat islands under 'ideal' conditions at night part 2: Diagnosis of causation // Boundary-Layer Meteorology. — 1991. — Vol. 56, no. 4. — P. 339–358. — https://doi.org/10.1007/BF00119211

Oke T. R. The energetic basis of the urban heat island // Quarterly Journal of the Royal Meteorological Society. — 1982. — Vol. 108, no. 455. — P. 1–24. — https://doi.org/10.1002/qj.49710845502

Rizwan A. M., Dennis L. Y. C. and Liu Ch. A review on the generation, determination and mitigation of Urban Heat Island // Journal of Environmental Sciences. — 2008. — Vol. 20, no. 1. — P. 120–128. — https://doi.org/10.1016/s1001-0742(08)60019-4

Scott A. A., Waugh D. W. and Zaitchik B. F. Reduced Urban Heat Island intensity under warmer conditions // Environmental Research Letters. — 2018. — Vol. 13, no. 6. — P. 064003. — https://doi.org/10.1088/1748-9326/aabd6c

Sobstyl J. M., Emig T., Abdolhosseini Qomi M. J., et al. Role of City Texture in Urban Heat Islands at Nighttime // Physical Review Letters. — 2018. — Vol. 120, no. 10. — P. 108701. — https://doi.org/10.1103/PhysRevLett.120.108701

Stempihar J. J., Pourshams-Manzouri T., Kaloush K. E., et al. Porous asphalt pavement temperature effects for urban heat island analysis // Transportation Research Record: Journal of the Transportation Research Board. — 2012. — Vol. 2293, no. 1. — P. 123–130. — https://doi.org/10.3141/2293-15

Stewart I. D., Krayenhoff E. S., Voogt J. A., et al. Time evolution of the surface urban heat island // Earth's Future. — 2021. — Vol. 9, no. 10. — https://doi.org/10.1029/2021EF002178

Stewart I. D. and Oke T. R. Local climate zones for urban temperature studies // Bulletin of the American Meteorological Society. — 2012. — Vol. 93, no. 12. — P. 1879–1900. — https://doi.org/10.1175/bams-d-11-00019.1

Tan J., Zheng Y., Tang X., et al. The urban heat island and its impact on heat waves and human health in Shanghai // International Journal of Biometeorology. — 2009. — Vol. 54, no. 1. — P. 75–84. — https://doi.org/10.1007/s00484-009-0256-x

Varentsov M., Fenner D., Meier F., et al. Quantifying Local and Mesoscale Drivers of the Urban Heat Island of Moscow with Reference and Crowdsourced Observations // Frontiers in Environmental Science. — 2021. — Vol. 9. — https://doi.org/10.3389/fenvs.2021.716968

Wen C., Mamtimin A., Feng J., et al. Diurnal Variation in Urban Heat Island Intensity in Birmingham: The Relationship between Nocturnal Surface and Canopy Heat Islands // Land. — 2023. — Vol. 12, no. 11. — P. 2062. — https://doi.org/10.3390/land12112062

Xue J., Zong L., Yang Y., et al. Diurnal and interannual variations of canopy urban heat island (CUHI) effects over a mountain-valley city with a semi-arid climate // Urban Climate. — 2023. — Vol. 48, no. 101425. — P. 101425. — https://doi.org/10.1016/j.uclim.2023.101425

Yoshino M. M. Climate in a small area: an introduction to local meteorology. — Tokyo : University of Tokyo Press, 1975. — 549 p.